Joint Design of Radar Transmit Waveform and Mismatched Filter with Low Sidelobes

Yang Jing[1], Junli Liang[1], Sergiy A. Vorobyov[2], Xuhui Fan[1], and Deyun Zhou[1]
[1]Electronics and Information, Northwestern Polytechnical University, Xi'an, 710072, China
[2]Department of Signal Processing and Acoustics, Aalto University, Espoo, 15400, Finland
Emails: jingyang@mail.nwpu.edu.cn, liangjunli@nwpu.edu.cn, sergiy.vorobyov@aalto.fi
fanxuhui@mail.nwpu.edu.cn, dyzhou@nwpu.edu.cn

***Abstract*— The paper focuses on joint design of transmit waveform and mismatched filter to achieve low sidelobe level for improving the resolution of pulse compression (PC). An L_p-norm, $p \geq 1$, of the power ratio of sidelobe to mainlobe levels is used in the corresponding PC optimization problem as a metric. The use of L_p-norm minimization contains as special cases the integrated sidelobe level and peak sidelobe level (PSL) minimization problems which corresponds to specific selections of different p values. The main contribution of this work is the development of a new iterative algorithm to solve the aforementioned optimization problem. It is based on using Dinkelbach's scheme together with majorization minimization method. The computational complexity of the proposed algorithm is also analyzed. Numerical examples demonstrate that waveforms and mismatched filters designed by using the proposed method produce lower PSL than the existing counterparts.**

***Index Terms*—Transmit waveform; receive filter; sidelobe levels; Dinkelbach algorithm; majorization minimization**

I. Introduction

The problem of sidelobe suppression has been attracting a lot of research attention because it enables to improve resolution of pulse compression (PC) in radar detection. In general, optimization of mismatched filter [1] and design of transmit waveforms [2] are two ways to suppress sidelobes. With respect to the mismatched filter design, several methods have been developed in the last decade. The method of Lagrange multipliers presented in [1] minimizes the L_p-norm of the sidelobe energies. In [3] and [4], the second-order cone programming (SOCP)-based formulations for sidelobe suppression problem have lead to some efficient methods. With respect to the transmit waveform design, iterative approaches for waveform design with low autocorrelation (AC) sidelobes have been suggested. Among such approaches are the cyclic algorithm new (CAN) [5], majorization minimization-based integrated sidelobe level (MISL) approach [6], [7], a heuristic approach based on the coordinate descent (CD) [8], and Lagrange programming neural network-alternating direction method of multipliers (LPNN-ADMM) [9].

This work was supported in part by the China Scholarship Council; in part by the Innovation Foundation for Doctor Dissertation of Northwestern Polytechnical University; in part by the Natural Science Foundation of China under Grant 61471295; in part by the Central University Funds under Grant G2016KY0308, G2016KY0002, and 17GH030144; and in part by Academy of Finland under Grants 299243 and 319822.

Joint design of transmit waveform and mismatched filter is an alternative way to reduce sidelobes. In [10] and [11], gradient descent-based methods for joint transmit waveform and receive mismatched filter design have been developed to minimize the peak sidelobe level (PSL).

To enrich the study on joint design of transmit waveform and mismatched filter and provide alternative and efficient methods, we develop here a joint design method with an objective of minimizing either integrated sidelobe level (ISL) or PSL. Our joint design problem is first formulated where an L_p-norm, $p \geq 1$, of the power ratio of sidelobe to mainlobe levels is used, which contains as special cases both ISL, for $p = 1$, and PSL, for $p = \infty$, minimization objectives. Then a new iterative algorithm is proposed to solve the L_p-norm problem of joint transmit waveform and mismatched filter design by employing the Dinkelbach's algorithm [12] and majorization minimization (MM) method [13]. In addition, we investigate the computational complexity of the proposed algorithm. Finally, we demonstrate the efficiency of the proposed method in terms of simulation examples.

Notations: Boldface uppercase and lowercase letters represent the matrices and vectors, while standard letters denote scalars. The notations $(\cdot)^*, (\cdot)^T$, and $(\cdot)^H$ are used for the conjugate, transpose, and conjugate transpose operations, respectively. Moreover, $\mathrm{tr}(\cdot)$ and $\mathrm{vec}(\cdot)$ denote the trace and matrix vectorization operators, respectively, while $|\cdot|$ stands for the absolute value of a real-valued scalar or the modulus of a complex number, or the elements number of a set. The notation $\|\cdot\|$ is reserved for the L_2 norm of a matrix (Frobenius norm) or a vector, $a^+ = \max\{a, 0\}$ and $a^- = \min\{a, 0\}$ for the real-valued variable a. Finally, $\mathbb{C}^{m\times n}$ denotes the $m \times n$ complex matrix space, $j = \sqrt{-1}$ is reserved for imaginary one, $\Re\{\cdot\}$ denotes the real part of a complex variable, $\mathbf{I}_n$ stands for the identity matrix of size $n \times n$, and $\mathbf{O}_{m\times n}$ represents the matrix of all zeros of size $m \times n$.

II. Problem Formulation

Let $\mathbf{x} = [x(1), \cdots, x(N)]^T$ and $\mathbf{h} = [h(1), \cdots, h(M)]^T$ denote the transmit waveform of length N and the vector of receive mismatched filter coefficients of length M. These will be our design variables throughout the paper. The integer numbers N and M should satisfy the equality $M = N + 2L$

where $L \geq 0$ [3]. The correlation r_l between $\mathbf{x}$ and $\mathbf{h}$ is given by $r_l = \mathbf{h}^H \mathbf{J}_l \mathbf{x},\ l = 0, \cdots, \pm(N+L-1)$, where $\mathbf{J}_l$ is an $M \times N$ matrix with the (m,n)th entry being

$$\mathbf{J}_l(m,n) = \begin{cases} 1 & \text{if } n = m + l - L \\ 0 & \text{otherwise} \end{cases}. \tag{1}$$

Then the PC of $\mathbf{x}$ and $\mathbf{h}$ is $|r_l|^2$.

For the discrete time delay set $\Omega \subseteq \{-(N+L-1), \cdots, -1, 1, \cdots, N+L-1\}$, the ISL, PSL and L_p-norm of the power ratio of sidelobe to mainlobe levels are the three commonly used metrics to measure the sidelobe level of PC. They are given respectively by

$$\sum_{l \in \Omega} \left(\frac{|\mathbf{h}^H \mathbf{J}_l \mathbf{x}|^2}{|\mathbf{h}^H \mathbf{J}_0 \mathbf{x}|^2} \right) \tag{2}$$

$$\max_{l \in \Omega} \left(\frac{|\mathbf{h}^H \mathbf{J}_l \mathbf{x}|^2}{|\mathbf{h}^H \mathbf{J}_0 \mathbf{x}|^2} \right) \tag{3}$$

and

$$\left(\sum_{l \in \Omega} \left(\frac{|\mathbf{h}^H \mathbf{J}_l \mathbf{x}|^2}{|\mathbf{h}^H \mathbf{J}_0 \mathbf{x}|^2} \right)^p \right)^{1/p}, \tag{4}$$

where $p \geq 1$ [1], [3].

Note that:

1) The power ratio of sidelobe level to mainlobe level is used in all three metrics.
2) If $p = 1$, (4) is equivalent to the ISL metric, while (4) is equivalent to the PSL metric if $p = +\infty$. Thus, different values of $p \in [1, +\infty)$ lead to different tradeoffs between ISL and PSL. The latter means that (4) is a generalized metric.
3) If (4) achieves its minimum value at the point $\mathbf{h}^\star$, the minimum can be also achieved at the point $ke^{j\theta}\mathbf{h}^\star$ for arbitrary real values $k \neq 0$ and θ. In other words, the minimum of (4) is unique only up to a scalar multiplication and phase rotation. To avoid the scale ambiguity, we let $\|\mathbf{h}\|^2 = \alpha$ with $\alpha > 0$ being the filter's power.
4) The constant modulus constraints $|x_n| = \beta$ $(\beta > 0)$, $n = 1, \cdots, N$ are required to maximize the efficiency of radar amplifier.

Now we can formulate the joint design problem of the matched filter and transmit waveform as follow:

$$\begin{aligned} \min_{\mathbf{x},\mathbf{h}} \ & \frac{\sum_{l \in \Omega} |\mathbf{h}^H \mathbf{J}_l \mathbf{x}|^{2p}}{|\mathbf{h}^H \mathbf{J}_0 \mathbf{x}|^{2p}}, \\ \text{s.t.} \ & |x_n| = \beta, n = 1, \cdots, N, \\ & \|\mathbf{h}\|^2 = \alpha. \end{aligned} \tag{5}$$

Let $\mathbf{y} \triangleq \begin{bmatrix} \mathbf{h} \\ \mathbf{x} \end{bmatrix} \in \mathbb{C}^{(M+N)\times 1}$. We can then write r_l as:

$$r_l = \mathbf{y}^H \tilde{\mathbf{J}}_l \mathbf{y},\ l = 0, \cdots, \pm(N+L-1), \tag{6}$$

and thus, the optimization problem (5) can be expressed as

$$\begin{aligned} \min_{\mathbf{y}} \ & g(\mathbf{y}) \\ \text{s.t.} \ & |y(n+M)| = \beta, n = 1, \cdots, N, \\ & \sum_{n=1}^{M} |y(n)|^2 = \alpha \end{aligned} \tag{7}$$

where the objective $g(\mathbf{y})$ becomes $g(\mathbf{y}) = \frac{\sum_{l \in \Omega} |\mathbf{y}^H \tilde{\mathbf{J}}_l \mathbf{y}|^{2p}}{|\mathbf{y}^H \tilde{\mathbf{J}}_0 \mathbf{y}|^{2p}} \geq 0$ with $\tilde{\mathbf{J}}_l$ denoting $\tilde{\mathbf{J}}_l = \begin{bmatrix} \mathbf{O}_{M\times M} & \mathbf{J}_l \\ \mathbf{O}_{N\times M} & \mathbf{O}_{N\times N} \end{bmatrix} \in \mathbb{R}^{(M+N)\times(M+N)}$, $l = 0, \cdots, \pm(N+L-1)$.

III. Proposed Algorithm

In this section, we develop an efficient algorithm for solving problem (7) based on Dinkelbach algorithm [12], [14], [15] and MM method. We name it as iterative majorization Dinkelbach's algorithm (IMDA). We also analyze the computational complexity of the proposed IMDA and explain how to accelerate it by using the squared iterative method (SQUAREM) [16].

Dinkelbach's algorithm is a superlinearly convergent method developed for fractional programming problems with nonincreasing monotonic objectives just like our problem (7). It is an iterative algorithm, and applied to (7), it leads to the following t-th iteration:

$$\begin{aligned} \min_{\mathbf{y}} \ & \tilde{g}_t(\mathbf{y}) \\ \text{s.t.} \ & |y(n+M)| = \beta, n = 1, \cdots, N, \\ & \sum_{n=1}^{M} |y(n)|^2 = \alpha \end{aligned} \tag{8}$$

where $\tilde{g}_t(\mathbf{y}) = \sum_{l \in \Omega} |\mathbf{y}^H \tilde{\mathbf{J}}_l \mathbf{y}|^{2p} - k^{\{t\}} |\mathbf{y}^H \tilde{\mathbf{J}}_0 \mathbf{y}|^{2p}$ with $k^{\{t\}}$ being updated as

$$k^{\{t\}} = \frac{\sum_{l \in \Omega} |(\mathbf{y}^{\{t\}})^H \tilde{\mathbf{J}}_l \mathbf{y}^{\{t\}}|^{2p}}{|(\mathbf{y}^{\{t\}})^H \tilde{\mathbf{J}}_0 \mathbf{y}^{\{t\}}|^{2p}} \geq 0. \tag{9}$$

Since problem (8) is still non-convex, the MM method is used to solve it. Particularly, for the problem $\min_x \ f(x)$ s.t. $x \in \mathcal{X}$, $\tilde{f}(x, x^\natural)$ is a "majorizer" of the function $f(x)$ at the point $x^\natural$ if it satisfies $\tilde{f}(x, x^\natural) \geq f(x)$, $x \in \mathcal{X}$, and $\tilde{f}(x^\natural, x^\natural) \geq f(x^\natural)$. One key step of MM is to find a "majorizer" problem. The latter can be constructed by using the following lemmas.

Lemma 1. (*Lemma 1 in [6]*): *Let $N \times N$ matrices $\mathbf{L}$ and $\mathbf{M}$ be Hermitian such that $\mathbf{M} \succeq \mathbf{L}$. Then for any point $\mathbf{x}_0 \in \mathbb{C}^N$, the "majorizer" of quadratic function $\mathbf{x}^H \mathbf{L} \mathbf{x}$ at the point $\mathbf{x}_0$ is given by*

$$\mathbf{x}^H \mathbf{M} \mathbf{x} + 2\Re\{\mathbf{x}^H (\mathbf{L} - \mathbf{M}) \mathbf{x}_0\} + \mathbf{x}_0^H (\mathbf{M} - \mathbf{L}) \mathbf{x}_0. \tag{10}$$

Lemma 2. (*Lemma 1 in [17]*): *The "majorizer" of $f(x) = x^q$ with integer $q \geq 2$ and $x \in [0, \mu]$ at $\forall x_0 \in [0, \mu)$ is given as*

$$ax^2 + 2bx + c \tag{11}$$

where $a = \frac{\mu^q - x_0^q - qx_0^{q-1}(\mu - x_0)}{(\mu - x_0)^2}$, $b = qx_0^{q-1} - 2ax_0$, *and* $c = ax_0^2 - (q-1)x_0^q$.

Lemma 3. *For* $a = \frac{\mu^q - x_0^q - qx_0^{q-1}(\mu - x_0)}{(\mu - x_0)^2}$, $b = \frac{qx_0^{q-1}}{2} - ax_0$, *and integer* $q \geq 2$, *the inequality* $b \leq 0$ *holds if* $x_0 \in \left[0, \mu(\frac{2}{q})^{1/(q-2)}\right)$.

The proof is given by fairly straightforward calculations, and therefore is omitted here because of the space limitations.

Let i_t represent the i_t-th MM iteration and $r_l^{[i_t]} = (\mathbf{y}^{[i_t]})^H \tilde{\mathbf{J}}_l \mathbf{y}^{[i_t]}$, $n = 0, \cdots, \pm(N-1)$. The objective function of (8), $\tilde{g}_t(\mathbf{y})$, can be expressed as the following function with respect to r_l:

$$\sum_{l \in \Omega} |r_l|^{2p} - k^{\{t\}} |r_0|^{2p}. \tag{12}$$

Applying Lemma 2 for the first term of (12), we obtain

$$\sum_{l \in \Omega} |r_l|^{2p} \leq \sum_{l \in \Omega} (a_l^{[i_t]} |r_l|^2 + 2b_l^{[i_t]} |r_l| + c_l^{[i_t]}), \tag{13}$$

where $a_l^{[i_t]} = \frac{(\mu^{[i_t]})^{2p} - |r_l^{[i_t]}|^{2p} - 2p|r_l^{[i_t]}|^{2p-1}(\mu^{[i_t]} - |r_l^{[i_t]}|)}{(\mu^{[i_t]} - |r_l^{[i_t]}|)^2}$, $b_l^{[i_t]} = p|r_l^{[i_t]}|^{2p-1} - a_l^{[i_t]} |r_l^{[i_t]}|$, $c_l^{[i_t]} = a_l^{[i_t]} |r_l^{[i_t]}|^2 - (2p-1)|r_l^{[i_t]}|^{2p}$, $\mu^{[i_t]} > |r_l^{[i_t]}| p^{1/(2p-2)}$, and the equality is achieved at the point $r_l = r_l^{[i_t]}$, $l \in \Omega$.

Moreover, applying Lemma 1 twice for $|r_l|^2$, $l \in \Omega$, we obtain

$$\begin{aligned} |r_l|^2 \leq & \check{\lambda}_l \mathbf{y}^H \mathbf{y} + 2\Re\{\mathbf{y}^H (\check{\mathbf{J}}_l - \check{\lambda}_l) \mathbf{y}^{[i_t]}\} \\ & + (\mathbf{y}^{[i_t]})^H (\check{\lambda}_l - \check{\mathbf{J}}_l) \mathbf{y}^{[i_t]} + 2\hat{\lambda}_l (\alpha + N\beta)^2 + \hat{c} \\ = & 2\Re\{\mathbf{y}^H (\check{\mathbf{J}}_l - \check{\lambda}_l) \mathbf{y}^{[i_t]}\} + \check{c}, \end{aligned} \tag{14}$$

where $\check{\mathbf{J}}_l = (r_l^{[i_t]})^* \tilde{\mathbf{J}}_l + r_l^{[i_t]} \tilde{\mathbf{J}}_l^H$, $\check{\lambda}_l = 2|r_l^{[i_t]}|$, $\hat{c}$ and $\check{c}$ are constants, and the equality is achieved at the point $\mathbf{y} = \mathbf{y}^{[i_t]}$. Note also here that according to the inequality for $\mu^{[i_t]}$ below (13), $|r_l^{[i_t]}| \in \left[0, \frac{\mu^{[i_t]}}{p^{1/(2p-2)}}\right) \in \left[0, \mu^{[i_t]}\right)$ holds. The latter means that the inequality $b_l^{[i_t]} \leq 0$ holds due to Lemma 3.

Note that

$$|r_l| \geq \frac{1}{|r_l^{[i_t]}|} \Re\left\{(r_l^{[i_t]})^* r_l\right\}. \tag{15}$$

Multiplying both sides of (15) by $2b_l^{[i_t]}$, we obtain

$$2b_l^{[i_t]} |r_l| \leq \frac{2b_l^{[i_t]}}{|r_l^{[i_t]}|} \Re\left\{(r_l^{[i_t]})^* r_l\right\}. \tag{16}$$

For $l = 0, \cdots, \pm(N+L-1)$, let

$$\bar{\mathbf{J}}_l = \frac{b_l^{[i_t]}}{|r_l^{[i_t]}|} ((r_l^{[i_t]})^* \tilde{\mathbf{J}}_l + (r_l^{[i_t]}) \tilde{\mathbf{J}}_l^H), \ \bar{\lambda}_l = 2|b_l^{[i_t]}|. \tag{17}$$

Using the fact that $r_l = \mathbf{y}^H \tilde{\mathbf{J}}_l \mathbf{y}$, Lemma 1, and the fact that $\mathbf{y}^H \mathbf{y} = \alpha + N\beta$, we obtain

$$\begin{aligned} & 2b_l^{[i_t]} \Re\{(r_l^{[i_t]})^* r_l\} = \mathbf{y}^H \bar{\mathbf{J}}_l \mathbf{y} \\ \leq & \bar{\lambda}_l (\mathbf{y}^H \mathbf{y} + (\mathbf{y}^{[i_t]})^H \mathbf{y}^{[i_t]}) \\ & + 2\Re\{\mathbf{y}^H (\bar{\mathbf{J}}_l - \bar{\lambda}_l \mathbf{I}_{M+N}) \mathbf{y}^{[i_t]}\} - (\mathbf{y}^{[i_t]})^H \bar{\mathbf{J}}_l \mathbf{y}^{[i_t]} \\ = & 2\Re\{\mathbf{y}^H (\bar{\mathbf{J}}_l - \bar{\lambda}_l \mathbf{I}_{M+N}) \mathbf{y}^{[i_t]}\} + \bar{c}_n, \end{aligned} \tag{18}$$

where $\bar{c}_n$ is a constant. Thus, ignoring the constant terms, the "majorizer" of $2b_l^{[i_t]} |r_l|$ at the point $\mathbf{y}^{[i_t]}$ can be found to be

$$2\Re\{\mathbf{y}^H (\bar{\mathbf{J}}_l - \bar{\lambda}_l \mathbf{I}_{M+N}) \mathbf{y}^{[i_t]}\}. \tag{19}$$

The second term of (12) is concave since $|r_0|^{2p}$ is convex and $k^{\{t\}} \geq 0$. Using the first order Taylor's expansion of the concave function $-k^{\{t\}} |r_0|^{2p}$, we obtain

$$\begin{aligned} & - k^{\{t\}} |r_0|^{2p} \\ \leq & - k^{\{t\}} |r_0^{[i_t]}|^{2p} - 2pk^{\{t\}} |r_0^{[i_t]}|^{2(p-1)} \Re\{(r_0^{[i_t]})^* (r_0 - r_0^{[i_t]})\} \\ = & (2p-1) k^{\{t\}} |r_0^{[i_t]}|^{2p} + 2b_0^{[i_t]} \Re\{(r_0^{[i_t]})^* r_0\}, \end{aligned} \tag{20}$$

where $b_0^{[i_t]} = -pk^{\{t\}} |r_0^{[i_t]}|^{2p-1} \leq 0$, and the equality is achieved at the point $r_l = r_l^{[i_t]}$. Similar to (18), ignoring the constant terms, a "majorizer" of $2b_0^{[i_t]} \Re\{(r_0^{[i_t]})^* r_0\}$, and thus, a "majorizer" of $-k^{\{t\}} |r_0|^{2p}$ at the point $\mathbf{y}^{[i_t]}$ is given by

$$2\Re\{\mathbf{y}^H (\bar{\mathbf{J}}_0 - \bar{\lambda}_0 \mathbf{I}_{M+N}) \mathbf{y}^{[i_t]}\}, \tag{21}$$

where $\bar{\mathbf{J}}_0$ and $\bar{\lambda}_0$ are defined in (17) for $l = 0$.

Combining (14) and (19) with (21) and again ignoring the constant terms, a "majorizer" of (13) at $\mathbf{y}^{[i_t]}$ is given by

$$\begin{aligned} \min_{\mathbf{y}} \ & -2\Re\{\mathbf{y}^H \hat{\mathbf{a}}^{[i_t]}\} \\ \text{s.t.} \ & |y(n+M)| = \beta, n = 1, \cdots, N, \\ & \sum_{n=1}^{M} |y(n)|^2 = \alpha, \end{aligned} \tag{22}$$

where

$$\begin{aligned} \hat{\mathbf{a}}^{[i_t]} = & \left(\bar{\lambda}_0 + \sum_{l \in \Omega} (a_l^{[i_t]} \check{\lambda}_l + \bar{\lambda}_l)\right) \mathbf{y}^{[i_t]} \\ & - \left(\bar{\mathbf{J}}_0 + \sum_{l \in \Omega} (a_l^{[i_t]} \check{\mathbf{J}}_l + \bar{\mathbf{J}}_l)\right) \mathbf{y}^{[i_t]}. \end{aligned} \tag{23}$$

Let $\hat{\mathbf{a}}_u^{[i_t]} = [\hat{a}^{[i_t]}(1), \cdots, \hat{a}^{[i_t]}(M)]^T$ and $\hat{\mathbf{a}}_d^{[i_t]} = [\hat{a}^{[i_t]}(M+1), \cdots, \hat{a}^{[i_t]}(M+N)]^T$. The closed-form solution to (22) can be then expressed as

$$\mathbf{y}^{[i_t+1]} = \begin{bmatrix} \hat{\mathbf{a}}_u^{[i_t]} / \|\hat{\mathbf{a}}_u^{[i_t]}\| \\ e^{j\angle(\hat{\mathbf{a}}_d^{[i_t]})} \end{bmatrix}. \tag{24}$$

The iterates (24) repeat until a stopping condition, for example, $\frac{\|\mathbf{y}^{[i_t+1]} - \mathbf{y}^{[i_t]}\|}{\|\mathbf{y}^{[i_t]}\|} < 10^{-3}$, is satisfied. Then $\mathbf{y}$ is updated as

$$\mathbf{y}^{\{t+1\}} = \mathbf{y}^{[i_t+1]} \tag{25}$$

followed by increasing t to $t+1$ and repeating (8)-(25) until stopping condition is satisfied.

A. The IMDA Flow

The flow of the proposed IMDA for solving (7) is as follows:

Flow of IMDA

Initialize: $t = 0$ and $\mathbf{y}^{\{0\}} = \begin{bmatrix} \mathbf{h}^{\{0\}} \\ \mathbf{x}^{\{0\}} \end{bmatrix}$. Assign values to the stopping criteria δ_o and δ_i, and the maximum number of iterations T_o.

Step 1: Update $k^{\{t\}}$ according to (9) and write the t-th iteration Dinkelbach problem of (7) according to (8).

Step 2: Use the MM method to solve (8):

- **Initialize:** $i_t = 0$ and $\mathbf{y}^{[0]} = \mathbf{y}^{\{t\}}$.
- **Step 2.1:** Calculate $\hat{\mathbf{a}}^{[i_t]}$ and $\mathbf{y}^{[i_t+1]}$ using (23) and (24), respectively.
- **Step 2.2:** If $\frac{\|\mathbf{y}^{[i_t+1]}-\mathbf{y}^{[i_t]}\|}{\|\mathbf{y}^{[i_t]}\|} \leq \delta_i$ is met, go to step 3; otherwise, increase i_t to $i_t + 1$ and go to step 2.1.

Step 3: Update $\mathbf{y}^{\{t+1\}} = \mathbf{y}^{[i_t+1]}$.

Stop and output $\mathbf{h} = [y^{\{t+1\}}(1), \cdots, y^{\{t+1\}}(M)]^T$ and $\mathbf{x} = [y^{\{t+1\}}(M+1), \cdots, y^{\{t+1\}}(M+N)]^T$ if $\frac{\|\mathbf{y}^{\{t+1\}}-\mathbf{y}^{\{t\}}\|}{\|\mathbf{y}^{\{t\}}\|} \leq \delta_o$ or $t \geq T_o$. Otherwise, increase t to $t + 1$ and go to Step 1.

B. Complexity

For each MM iteration of the proposed IMDA, the computational complexity is dominated by the number of flops required for updating $\hat{\mathbf{a}}^{[i_t]}$. As shown in (23), calculating $\hat{\mathbf{a}}^{[i_t]}$ requires computing $\check{\mathbf{J}}_l\mathbf{y}^{[i_t]}$, $\bar{\mathbf{J}}_l\mathbf{y}^{[i_t]}$, $r_l^{[i_t]}$, and $|r_l^{[i_t]}|^{2p}$. Operation $(\cdot)^{2p}$ requires about $2p\log_2(2p)$ flops, $\tilde{\mathbf{J}}_l\mathbf{y}$ and $\tilde{\mathbf{J}}_l^H\mathbf{y}$ require N and M flops, respectively, due to the fact that both matrices $\check{\mathbf{J}}_l$ and $\bar{\mathbf{J}}_l$ are linear combinations of $r_l^*\check{\mathbf{J}}_l$ and $r_l\tilde{\mathbf{J}}_l^H$ according to equations below (14) and (17). Then r_l requires about N flops. Therefore, the computational complexity of updating $\hat{\mathbf{a}}^{[i_t]}$ is $O(|\Omega|(M + 2p\log_2(2p)))$, which is the same as that for the methods in [10] and [11]. Moreover, the IMDA can be accelerated by using SQUAREM [16] which requires about $|\Omega|(M + 2p\log_2(2p)\bar{S})$ flops per MM iteration, where $\bar{S}$ is a mean iteration number of SQUAREM used.

IV. Numerical Examples

A. Effect of SQUAREM on the Convergence of the IMDA

First, we study the effect of SQUAREM on the convergence of the proposed IMDA. The proposed IMDA without SQUAREM-based acceleration is denoted as "IMDA-II" and with the acceleration as "IMDA-I".

We consider the transmit waveform $\mathbf{x}$ and mismatched filter $\mathbf{h}$ design of lengths $N = 128$ and $M = 256$, respectively, i.e., $L = 64$. Let $\alpha = N$ and $\beta = 1$. The sidelobe set is $\Omega = \{-(N + L - 1), \cdots, -1, 1, \cdots, N + L - 1\}$. The parameters of the IMDA are set as $p = 10$, $\delta_o = \delta_i = 10^{-5}$, and $T_o = 200$. The initial transmit waveform $\mathbf{x}^{\{0\}}$ is a Golomb sequence and the mismatched filter is initialized as $\mathbf{h}^{\{0\}} = [\mathbf{0}_{L\times 1}^T \ (\mathbf{x}^{\{0\}})^T \ \mathbf{0}_{L\times 1}^T]^T$.

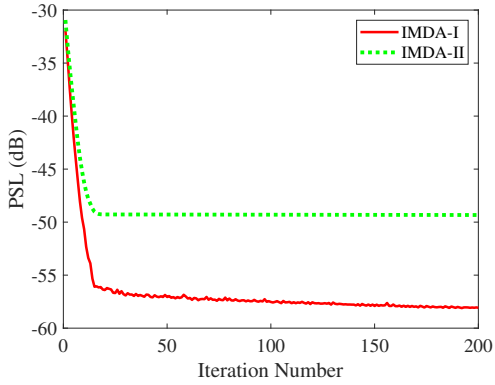

Fig. 1: Convergence and acceleration effect on the IMDA.

The results for the non-accelerated and accelerated implementations of the proposed IMDA are shown in Fig. 1 in terms of PSLs (for $p = 10$) versus number of iterations. It can be seen from the figure that both implementations of the proposed IMDA show convergence whether SQUAREM is used or not. However, IMDA-I converges faster than IMDA-II, and the achieved PSL by IMDA-I (-58.07dB) is lower than that of IMDA-II (-49.33dB). Therefore, the IMDA with SQUAREM-based acceleration is preferable, and we used only the implementation with acceleration in the next experiment.

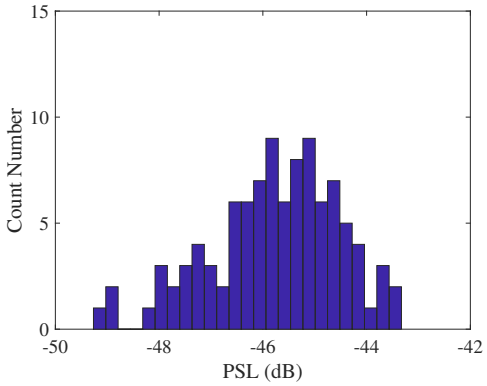

Fig. 2: Histogram of PSLs produced by the proposed IMDA.

B. Different Initializations

To investigate the sensitivity of the IMDA to different initializations, in this example, we run the IMDA for 100 Monte Carlo trials with unimodular sequence $\mathbf{x}^{(0)}$ of length $N = 128$ initialized by CAN [5]. The parameters of the IMDA are $p = 10$, $\delta_o = \delta_i = 10^{-5}$, and other parameters are set the same as those in Section IV-A. For comparison, we also run the methods proposed in [10] (with optimally selected parameters $\alpha = 0$, $\beta = 0.3$, $m = 20$, and $\mu = 2$) and [11] (with optimally selected parameters $\rho = 20$, $\mu = 5 \times 10^{-5}$, and pattern g is of -70dB PSL) with the same 100 initial CAN sequences.

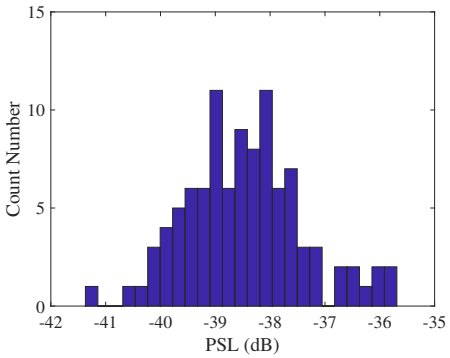

Fig. 3: Histogram of PSLs produced by the method of [10].

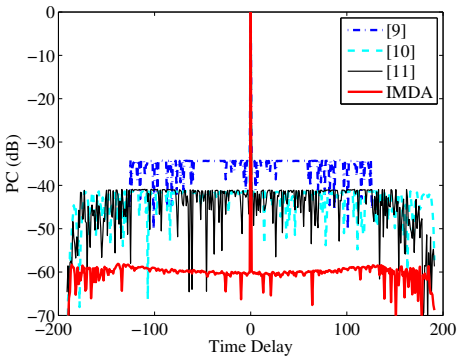

Fig. 5: PCs of the IMDA and methods of [9], [10], and [11].

The histograms of PSLs for different methods tested are plotted in Figs. 2-4. The histograms indicate that the PSLs corresponding to the transmit waveform and mismatched filter designed by the IMDA initialized for different initial CAN sequences are different. However, compared with the methods of [10] and [11], the IMDA produces lower PSLs.

Finally, we plot the PCs corresponding to the best PSLs of the three aforementioned methods and also the algorithm developed [9]. The results are shown in Fig. 5. It can be seen from the figure that PSL of the IMDA (-49.27dB) is significantly lower than that obtained by the algorithms proposed in [9] (-34.18dB), [10] (-41.37dB), and [11] (-40.88dB). A lower PSL can be obtained by choosing a good initialization, such as Golomb sequences shown in Section IV-A (-58.07dB).

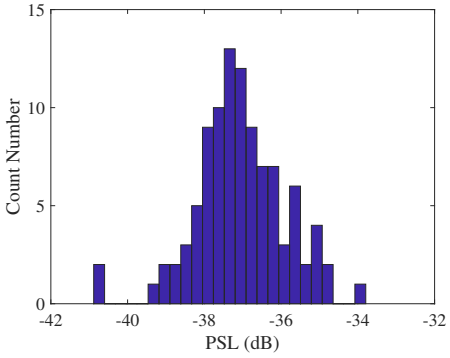

Fig. 4: Histogram of PSLs produced by the method of [11].

V. Conclusion

The joint transmit waveform and mismatched filter design problem has been considered here as the minimization of the L_p-norm of the power ratio of sidelobe to mainlobe levels. Since both ISL and PSL are special cases of our formulation, it can turn to ISL and PSL minimization flexibly. An efficient algorithm for solving this problem named as IMDA based on Dinkelbach's algorithm and MM method has been developed, and its efficiency has been demonstrated throughout simulation examples.

References

[1] J. E. Cilliers and J. C. Smit, "Pulse compression sidelobe reduction by minimization of L_p-norms," *IEEE Transactions on Aerospace and Electronic Systems*, vol. 43, no. 3, pp. 1238–1247, July 2007.

[2] J. Liang, H. C. So, J. Li, and A. Farina, "Unimodular sequence design based on alternating direction method of multipliers," *IEEE Transactions on Signal Processing*, vol. 64, no. 20, pp. 5367–5381, Oct 2016.

[3] A. De Maio, Y. Huang, M. Piezzo, S. Zhang, and A. Farina, "Design of radar receive filters optimized according to L_p-norm based criteria," *IEEE Transactions on Signal Processing*, vol. 59, no. 8, pp. 4023–4029, Aug 2011.

[4] P. J. Kajenski, "Mismatch filter design via convex optimization," *IEEE Transactions on Aerospace and Electronic Systems*, vol. 52, no. 4, pp. 1587–1591, August 2016.

[5] H. He, J. Li, and P. Stoica, *Waveform design for active sensing systems: a computational approach*. Cambridge University Press, 2012.

[6] J. Song, P. Babu, and D. P. Palomar, "Optimization methods for designing sequences with low autocorrelation sidelobes," *IEEE Transactions on Signal Processing*, vol. 63, no. 15, pp. 3998–4009, Aug 2015.

[7] Y. Li and S. A. Vorobyov, "Fast algorithms for designing multiple unimodular waveform(s) with good correlation properties," *IEEE Transactions on Signal Processing*, vol. 66, no. 5, pp. 1197–1212, Mar 2018.

[8] M. A. Kerahroodi, A. Aubry, A. De Maio, M. M. Naghsh, and M. Modarres-Hashemi, "A coordinate-descent framework to design low PSL/ISL sequences," *IEEE Transactions on Signal Processing*, vol. 65, no. 22, pp. 5942–5956, Nov 2017.

[9] Y. Jing, J. Liang, B. Tang, and J. Li, "Designing unimodular sequence with low peak of sidelobe level of local ambiguity function," *IEEE Transactions on Aerospace and Electronic Systems*, vol. 55, no. 3, pp. 1393–1406, June 2019.

[10] L. Xu, H. Liu, K. Yin, H. Zang, S. Zhou, and H. Wang, "Joint design of phase coded waveform and mismatched filter," in *2015 IEEE Radar Conference*, Oct 2015, pp. 32–36.

[11] U. Tan, O. Rabastc, C. Adnet, and J. .-. Ovarlez, "A sequence-filter joint optimization," in *2018 26th European Signal Processing Conference (EUSIPCO)*, Sep. 2018, pp. 2335–2339.

[12] W. Dinkelbach, "On nonlinear fractional programming," *Management science*, vol. 13, no. 7, pp. 492–498, 1967.

[13] D. R. Hunter and K. Lange, "A tutorial on MM algorithms," *The American Statistician*, vol. 58, no. 1, pp. 30–37, 2004.

[14] S. Schaible, "Fractional programming. II, on Dinkelbach's algorithm," *Management science*, vol. 22, no. 8, pp. 868–873, 1976.

[15] L. Wu and D. P. Palomar, "Sequence design for spectral shaping via minimization of regularized spectral level ratio," *IEEE Transactions on Signal Processing*, vol. 67, no. 18, pp. 4683–4695, Sep. 2019.

[16] R. Varadhan and C. Roland, "Simple and globally convergent methods for accelerating the convergence of any EM algorithm," *Scandinavian Journal of Statistics*, vol. 35, no. 2, pp. 335–353, 2008. [Online]. Available: http://www.jstor.org/stable/41548597

[17] J. Song, P. Babu, and D. P. Palomar, "Sequence design to minimize the peak sidelobe level," in *2016 IEEE International Conference on Acoustics, Speech and Signal Processing (ICASSP)*, March 2016, pp. 3896–3900.